MOLECULAR AND CELLULAR BIOLOGY, Oct. 1993, p. 6089–6101
0270-7306/93/106089-13$02.00/0

Vol. 13, No. 10

# NF-κB p100 (Lyt-10) Is a Component of H2TF1 and Can Function as an IκB-Like Molecule

ROBERT I. SCHEINMAN,[1] AMER A. BEG,[1,2] AND ALBERT S. BALDWIN, JR.[1,2]*

*Lineberger Comprehensive Cancer Center[1] and Department of Biology, CB No. 7295,[2] University of North Carolina at Chapel Hill, Chapel Hill, North Carolina 27599*

Received 18 December 1992/Returned for modification 26 February 1993/Accepted 2 July 1993

**NF-κB is an important transcription factor regulating expression of genes involved in immune function, inflammation, and cellular growth control. NF-κB activity is induced by numerous stimuli, such as phorbol esters, B- and T-cell mitogens, the cytokines tumor necrosis factor and interleukin-1, and serum growth factors. The standard model for the induction of NF-κB activity involves the release of the transcription factor from a cytoplasmic inhibitor termed IκB, allowing translocation of NF-κB to the nucleus. IκB contains multiple copies of the so-called ankyrin repeat, which are apparently necessary for its function. Subunits comprising NF-κB and related binding activities are members of the Rel multigene family. Two such subunits, p50 and p52 (also called p50B), are proteolytically processed from precursors of 105 kDa (also called p105 and NFKB1) and 100 kDa (also called p100, NFKB2, and Lyt-10), respectively. Both contain N-terminal Rel-homologous domains as well as multiple copies of C-terminal ankyrin repeats. We show here that NF-κB p100 is a component of the previously identified DNA-binding activity H2TF1. In addition, we show that p100 is localized in the cytoplasm in HeLa cells, where it is associated with c-Rel, p50, or p65 (RelA). In transient-transfection assays, p100 represses the ability of NF-κB p65 to activate a κB-containing reporter construct. Transfection of p100 also results in a loss of nuclear p65 DNA binding to a κB probe, as measured by an electrophoretic mobility shift assay, and a loss of nuclear p65 immunoreactivity, as measured by immunoblotting. This loss of nuclear p65 is paralleled by a gain of p65 DNA-binding activity and immunoreactivity in the cytoplasm. We interpret these data as demonstrating that p100 functions as an IκB-like molecule to sequester Rel family members in the cytoplasm. Proteolytic processing of p100 to the activator p52 is predicted to generate several new forms of Rel family heterodimers and therefore represents a form of regulation of NF-κB activity distinct from the classic IκB pathway.**

The transcription factor NF-κB, first described as a regulator of the immunoglobulin kappa (Ig κ) light-chain gene (38, 58), is now understood to play an important role as an activator of numerous genes of the immune and inflammation systems as well as of human immunodeficiency virus (HIV) gene transcription (4, 24, 38, 45). NF-κB activity, while constitutive in mature B cells, is rapidly induced by stimuli such as exposure to cytokines, mitogens, phorbol esters, reactive oxygen intermediates, and viral infection (4, 5, 38, 39, 57, 59). One mechanism by which this rapid induction of NF-κB activity is made possible is the storage of presynthesized NF-κB in the cytoplasm, bound to the inhibitor IκB (1, 2). While the mechanism by which NF-κB is liberated from its inhibitor is not well understood, in vitro data suggest that the phosphorylation of IκB markedly reduces its affinity for NF-κB subunits (22, 60). In addition, recent work has shown that multiple inducers of NF-κB lead to the phosphorylation of IκBα (8) and to the rapid loss of this inhibitor protein (8, 14, 63). Release from IκB unmasks the nuclear localization signal for NF-κB, allowing it to translocate to the nucleus, where it may then bind to a family of related DNA-binding sites (9).

The best studied form of NF-κB consists of a heterodimer of a 50-kDa (p50) and a 65-kDa (p65 [RelA]) subunit (3, 33). The cloning of the cDNAs encoding these subunits has shown that they are both homologous with the c-*rel* protooncogene and with the *Drosophila* maternal-effect gene *dorsal* (12, 23, 35, 50, 54). In addition, the cloning of p50 revealed that it is derived from the N terminus of a 105-kDa precursor (p105 [NFKB1]) via an ATP-dependent proteolytic pathway (20). Deletion studies have shown that DNA binding is detectable only after removal of the C-terminal portion of p105 (23, 35). This C-terminal region of p105 contains an interesting repeat structure of conserved elements found both in erythrocyte ankyrin and in several cell cycle control proteins (23, 35). p50, p65, and c-Rel contain an N-terminal Rel-homologous region which contributes dimerization, nuclear localization, and DNA-binding domains to these proteins (9, 24, 28, 50). Homodimers of p50 and of p65 as well as heterodimers of c-Rel with either p50 or p65 can bind κB sites (25, 35, 50, 54, 64). Characterization of these dimers has revealed that each has its own subset of preferred DNA-binding sites within the κB consensus sequence (25, 37). In addition, recent studies have shown the association of the p105 precursor with c-Rel, p50, and p65 (16, 44, 46, 53). This suggests that NF-κB subunits may be part of a complex regulatory network in which different subsets of genes might be activated by different dimeric combinations of Rel and NF-κB subunits.

The retention of NF-κB and Rel proteins in the cytoplasm is mediated by a family of related proteins referred to collectively as IκB. Multiple forms of IκB have been cloned, including IκBα/MAD-3, its chicken homolog pp40, Bcl-3, and IκBγ (26, 27, 30, 34). Strikingly, each form of IκB contains multiple copies of ankyrin repeats highly similar to those of p105 (19, 26). Deletion studies have shown that these ankyrin repeats play a crucial role in the inhibition of DNA binding (31).

The high degree of conservation of the *rel* homology

* Corresponding author.

domain led a number of laboratories to search for other *rel*-related genes. A cDNA similar to that encoding p105 was thus identified and named p100 (also referred to as p98 and NFKB2) (43, 56). Interestingly, the gene encoding this protein was also identified by the sequencing of the (10; 14)(q24;q32) translocation breakpoint associated with certain B-cell leukemias and named *lyt*-10 (47). Additionally, p100 (Lyt-10) was identified in a library of mitogen-induced genes (10). Sequence comparisons of *rel* family members show that p100 is most closely related to p105. Both proteins contain an N-terminal Rel homology domain, nuclear localization sequences, and C-terminal ankyrin repeats (43, 47, 56). Like p105, p100 is a precursor protein which is processed to a 52- to 55-kDa protein (p52) (43). N-terminal truncations of p100 have been shown to bind to p50, p65, and c-Rel and, when heterodimerized with p65, to activate gene transcription in transient-transfection assays (43, 52, 56). The potentially oncogenic form of p100 (Lyt-10) is fused to the immunoglobulin Cα gene, resulting in a chimera which retains the Rel homology domain but has lost the C-terminal ankyrin repeats. Unlike p100, this chimera readily binds to the κB DNA motif in vitro (47). While the potential mechanism of oncogenesis through p100 is unknown, these data suggest that the C-terminal ankyrin repeats may play an important role in any growth-regulatory functions of this protein.

H2TF1 was identified in HeLa whole-cell extracts by its interaction with the region I enhancer of the murine *H-2K*$^b$ gene (6). This mode of identification suggested that H2TF1 plays a role in the regulation of major histocompatibility complex (MHC) gene expression. Initially, H2TF1 was identified in electrophoretic mobility shift assays (EMSAs) with a large fragment of the *H-2K*$^b$ promoter. This binding site was then localized to the region I enhancer by methylation interference (6). Both NF-κB and H2TF1 bind to this site, exhibiting a slightly different methylation interference pattern (7). The similarity in binding sites led to the concept that H2TF1 was possibly KBF1, recently identified as the NF-κB p50 homodimer. In this report, we identify a DNA-binding component of H2TF1 as the Rel family member p100. In addition, we show that p100 is localized to the cytoplasm and heterodimerizes with p50, p65, and c-Rel. Cytoplasmic p100 can repress gene activation mediated by p65 through its ability to sequester p65 in the cytoplasm. These properties suggest that p100 can function as an IκB. As p100 is proteolytically cleaved to give rise to p52, this predicts the formation of several new heterodimeric forms of Rel/NF-κB subunits and suggests that proteolytic cleavage of NF-κB precursor molecules represents a mechanism of regulating NF-κB activity distinct from the classic IκB pathway.

## MATERIALS AND METHODS

**Cell culture.** HeLa cells were grown in spinner cultures in Eagle's minimal essential medium (suspension) with 2 mM glutamine, 5% fetal calf serum, 5% horse serum, 100 U of penicillin per ml, and 100 μg of streptomycin per ml. Cell densities were kept between $2 \times 10^5$ and $1 \times 10^6$/ml during culture, and cells were harvested at a density of $5 \times 10^5$ to $1 \times 10^6$/ml for the preparation of extracts.

COS cells were maintained in Iscove's Dulbecco's modified Eagle's medium with 5 mM glutamine, 7.5% fetal calf serum, 100 U of penicillin per ml, and 100 μg of streptomycin per ml and passaged every 3 to 4 days. After passage 15, the cells were discarded.

TABLE 1. κB sites used in this study

| Enhancer | Sequence | Strand |
|---|---|---|
| MHC RI | TGGGGATTCCCCA | + |
| $\beta_2$-Microglobulin | AGGGACTTTCCCA | − |
| MHC $RII_a$ | CTGGGCTTCCCCA | − |
| Ig κ | AGGGGACTTTCCG | + |
| HIV long terminal repeat | TGGGGACTTTCCA | + |
| c-*myc* | CGGGTTTTCCCCA | + |
| MHC mutant | TGCGGATTCCCGA | + |

**Extract preparation.** HeLa whole-cell extracts were prepared and partially purified by passage over a phosphocellulose column (6). The 0.35 M salt fraction was collected and is referred to as HeLa B. For studies comparing cytoplasmic and nuclear proteins, cells were washed in phosphate-buffered saline (PBS) and lysed in E buffer (0.3% Nonidet P-40 [NP-40], 10 mM Tris [pH 8.0], 60 mM NaCl, 1 mM EDTA, 1 mM dithiothreitol, 1 mM phenylmethylsulfonyl fluoride) by 5 min of incubation on ice. Nuclei were pelleted by spinning for 5 min at 2,500 rpm at 4°C in an Eppendorf microcentrifuge, and the supernatant was saved as the cytoplasmic extract. Glycerol was added to cytoplasmic extracts to a final concentration of 20%, after which the extracts were stored at −80°C until use. Nuclei were washed in buffer E without NP-40 and resuspended in 100 μl of buffer C (20 mM HEPES [*N*-2-hydroxyethylpiperazine-*N*′-2-ethanesulfonic acid, pH 7.9], 0.75 mM spermidine, 0.15 mM spermine, 0.2 mM EDTA, 2 mM EGTA [ethylene glycol tetraacetic acid], 2 mM dithiothreitol, 20% glycerol, 1 mM phenylmethylsulfonyl fluoride). When mentioned, the nuclei were layered over a 0.5-ml sucrose pad and spun for 10 min at 2,500 rpm at 4°C in a desktop refrigerated centrifuge, and the pellet was resuspended in buffer C. NaCl was added to a concentration of 0.4 M, and the nuclei were gently shaken for 20 min at 4°C. The nuclei were then pelleted by spinning for 10 min at top speed at 4°C in an Eppendorf microcentrifuge, and the nuclear extract supernatant was stored at −80°C until use.

**DNA-binding reactions and EMSAs.** DNA sequences used as probes in EMSAs are shown in Table 1. These DNAs are derived from oligonucleotides cloned into the *Bam*HI site of a pUC polylinker and liberated by *Eco*RI and *Hin*dIII digestion. The DNA fragment containing the binding site was then purified on 1% low-melting-point agarose gels and labeled by a fill-in reaction with the Klenow fragment of DNA polymerase I and [α-$^{32}$P]dATP as described before (6). Additionally, some mobility shift assays were performed with a DNA probe designed for UV cross-linking studies. The synthesis of this probe is described below.

Binding reactions were performed by first incubating 5 to 10 μg of cell extract with 0.5 to 2 μg of poly(dI-dC) in binding buffer (10 mM Tris [pH 7.7], 50 mM NaCl, 20% glycerol, 1 mM dithiothreitol, 0.5 mM EDTA) for 10 min at room temperature. Approximately 10,000 cpm (0.2 ng) of probe was then added and allowed to bind for approximately 30 min. The reaction mix was then loaded onto native 5% acrylamide gels, prepared with either TAE (6.7 mM Tris, 3.3 mM sodium acetate, 1 mM EDTA, pH adjusted to 7.9) or 0.25× TBE (22.3 mM Tris, 22.3 mM borate, 0.5 mM EDTA). We have found that TAE gels are necessary to visualize non-cross-linked H2TF1 by EMSA. Supershift experiments were performed by incubating binding reaction mixes with 1 μl of antiserum for 15 min at room temperature. Gels were

analyzed either by autoradiography or with a PhosphorImager (Molecular Dynamics).

**UV cross-linking.** Two template oligonucleotides were synthesized, UV1 (CAGGGCTGGGGATTCCCCATCTCC ACAGTTTCACTTC) and UV3 (CAGGGCTGCGGATT CCCGATCTCCACAGTTTCACTTC), along with primer UV2 (GAAGTGAAACTGTGG). UV1 corresponds to bases −178 to −141 of the region I enhancer of the *H-2K*$^b$ gene, which contains a strong κB motif (7). UV2 and UV1 were annealed to form UV21 and extended with Klenow fragment in the presence of bromodeoxyuridine and [α-$^{32}$P]dCTP as described before (17). UV2 and UV3 were annealed and extended as above to make UV23, a mutant probe analogous to the MHC mutant probe (Table 1). Approximately 50 μg of cell extract was incubated for 10 min with 2 μg of poly(dI-dC) in binding buffer, and $2 \times 10^5$ to $1.5 \times 10^6$ cpm of probe was added to a final volume of 40 μl in a 1.5-ml microcentrifuge tube. The reaction was allowed to bind for 30 min at room temperature. It was then placed in a rack in the cold room so that a 302-nm UV light box could be placed directly on top of the open microcentrifuge tube. In this fashion, the binding reaction mix was irradiated with UV light for times ranging from 15 to 90 min. Cross-linked material was then analyzed either by sodium dodecyl sulfate-polyacrylamide gel electrophoresis (SDS-PAGE) or by mobility shift assay.

**Partial proteolysis.** Incomplete proteolysis of H2TF1 was achieved with the endoproteinase Glu-C (V8 protease). UV-irradiated binding reaction mixes were run on a native acrylamide gel (EMSA) to separate specific DNA-protein complexes. These complexes were located within the wet gel by autoradiography, and the bands were excised with a razor blade. The gel slices were then equilibrated with SDS loading buffer by boiling for 5 min and loaded onto a 10% acrylamide–SDS gel with a 5% acrylamide stacking gel. These samples were then overlaid with 25 μl of V8 protease (0 to 250 ng) in dilution buffer (250 mM Tris [pH 6.8], 0.1% SDS, 1 mM EDTA, 10% glycerol, 40 mM 2-mercaptoethanol, 0.005% bromophenol blue). When all proteins were focused in the stacking gel, the power was shut off for 10 to 30 min to allow the V8 to partially digest the proteins present, as described before (18, 21). The power was then restored, the gel was run to completion and dried, and DNA-cross-linked proteins were visualized by autoradiography.

**Antibodies and immunoprecipitations.** Ab2, a gift of A. Israel, is a polyclonal antiserum raised against the p50 subunit as described before (35). This antiserum recognizes p50 homodimers (KBF1) and p50-p65 heterodimers (NF-κB). Ab22, a gift of M. Karin, is a polyclonal antipeptide antiserum raised against a peptide encoding amino acids 1 to 14 of p105/p50 and has a higher avidity for p50 homodimers than p50 heterodimers (43). Ab9 is a polyclonal antiserum raised against a peptide encoding amino acids 6 to 20 of IκBα/MAD-3. Ab9 recognizes IκB but not p50 or p65 in immunoprecipitation assays (9). Ab265, a gift of N. Rice, is a polyclonal antipeptide antiserum specific for human c-Rel, prepared as described before (15). Ab1101 is a polyclonal antiserum raised against a peptide encoding amino acids 1 to 21 of p65. Ab2932, a gift of M. Karin, is a polyclonal antipeptide antiserum raised against a peptide (peptide 2932) encoding amino acids 1 to 19 of p100 (Lyt-10) and has a higher avidity for p100 homodimers than for p100 heterodimers (43).

Immunoprecipitations of cross-linked proteins were performed by combining a 40-μl cross-linked binding reaction mix (containing $5 \times 10^5$ cpm of freshly synthesized UV21 probe and 5 μl of HeLa cell extract) with 400 μl of RIP buffer (25 mM Tris [pH 7.6], 150 mM NaCl, 2 mM EDTA, 1 mM phenylmethylsulfonyl fluoride, 0.5% NP-40) and 1 to 2 μl of antiserum. For some immunoprecipitations, 4.4 μl of 10% SDS was added to cross-linked binding reaction mixes and the samples were boiled for 5 min to abolish protein-protein interactions. Antiserum and 400 μl of RIP buffer were then added. Reaction mixes were rotated for 30 min at 4°C. The samples were then transferred to tubes containing a 1:1 slurry of protein A-Sepharose (PAS) in PBS plus 1% bovine serum albumin and rotated for 60 min at 4°C. The PAS was then washed twice in each of the following buffers as described before (62): (i) 1 M NaCl, 20 mM Tris (pH 7.6), plus 0.1% NP-40; (ii) 0.2 M NaCl, 20 mM Tris (pH 7.6), and 1% NP-40; (iii) 20 mM Tris (pH 7.6) plus 0.1% NP-40; and (iv) 50 mM Tris (pH 6.8). The pellet was then resuspended in 100 μl of SDS-PAGE loading buffer, boiled for 5 min loaded, and run on 7% acrylamide–SDS gels.

$^{35}$S-labeled HeLa cell extracts were immunoprecipitated by combining 2 to 5 μl of antibody with 100 to 200 μl of extract and processed as above. For PAS elution experiments, $^{35}$S-labeled HeLa cell extracts were immunoprecipitated, and PAS pellets, washed as described above, were incubated overnight in 200 μl of RIP buffer containing 50 μg of peptide 2932 per ml as described before (36). The supernatant was then collected and reimmunoprecipitated with a different antibody, and new PAS was added and washed as above. The pellets were resuspended in 100 μl of SDS-PAGE loading buffer plus 10 μg of bovine serum albumin as a carrier, boiled for 5 min, and analyzed by SDS-PAGE.

**$^{35}$S labeling of HeLa cells.** HeLa cells were grown to a density of $10^7$ cells per 35-mm-diameter plate in Dulbecco's modified Eagle's medium without methionine for 1 h, after which [$^{35}$S]methionine (Translabel; ICN) was added to 500 μCi/ml. Cells were incubated for 2 h, harvested, placed on ice, and washed with PBS. The cells were then lysed with 1 ml of RIP buffer on ice for 5 min and spun at 14,000 rpm for 10 min at 4°C. Immunoprecipitations were typically performed on 100 to 200 μl of extract. Nuclear and cytoplasmic extracts were prepared as described above except that after cell lysis, washed nuclei were boiled for 5 min in 44 μl of E buffer plus 1% SDS; 400 μl of RIP buffer was then added, and immunoprecipitations were performed as described above.

**Transfections, CAT assays, and protein assays.** HeLa cells were transfected by electroporation with the Bio-Rad Gene Pulser with a capacitance extender. Approximately $3 \times 10^6$ to $1 \times 10^7$ cells were transfected in a volume of 0.5 ml at a setting of 300 V and 960 μF in a 0.4-cm gapped cuvette. Transfected samples were transferred to 25-cm$^2$ flasks in 10 ml of medium and incubated at 37°C for 16 to 24 h. COS cells were transfected by the DEAE-dextran method (32). Cells were harvested after 48 h, and chloramphenicol acetyltransferase (CAT) activity was determined as described before (48). The data were normalized to input protein levels, assayed by the method of Bradford (13) with Bio-Rad dye reagent according to the manufacturer's instructions.

**Immunoblots.** Extracts were run through SDS–10% PAGE gels and electroblotted to nitrocellulose filters in 0.025 M Tris base–0.2 M glycine–20% methanol at 100 V for 1 h at 4°C. The nitrocellulose was blocked for 30 min in 1% bovine serum albumin in TBST (10 mM Tris, 150 mM NaCl, or 0.05% Tween 20). Antiserum 1101, specific for p65, was diluted 1:2,000 in TBST. Blots were shaken for 30 min in diluted antiserum and washed three times in TBST. Fluorescein isothiocyanate-conjugated anti-rabbit immunoglobulin

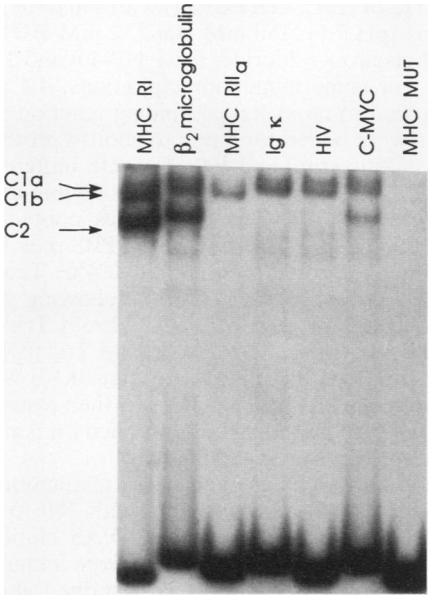


FIG. 1. Binding specificity of H2TF1. A phosphocellulose fraction of a HeLa whole-cell extract was incubated with the labeled DNA fragments listed in Table 1. The binding reaction mixes were then analyzed on a TAE–5% acrylamide native gel, which was subsequently dried and visualized by autoradiography. Complexes C1a, C1b, and C2 are indicated by the arrows. The labeled DNA fragment present in the binding reaction mix is indicated over each lane.

G (Promega) was diluted 1:7,500. Blots were incubated for 30 min in diluted secondary antibody and washed three times in TBST. Immunoreactivity was visualized by alkaline phosphatase color reaction with the ProBlot kit (Promega) according to the manufacturer's instructions.

## RESULTS

**Binding specificity of H2TF1.** H2TF1 was originally identified by its ability to bind to a site in the region I enhancer of the *H-2K*$^b$ MHC class I gene (6). NF-κB binds to this same region with high affinity, competes with H2TF1 for binding in vitro, and generates a methylation interference pattern closely related to that of H2TF1 (7). In order to better understand the sequence requirements for the binding of these two factors, we prepared a panel of NF-κB binding sites and tested them for binding to H2TF1. The HeLa B phosphocellulose fraction (6) of a HeLa whole-cell extract (from which H2TF1 was originally identified) was used as a source of H2TF1 for this experiment, and binding was assayed by mobility shift. The sequences used as DNA probes for this study are listed in Table 1.

The MHC region I enhancer binding site (MHC RI) was shifted as at least three complexes by proteins within the HeLa B fraction (Fig. 1, lane 1). The upper doublet will be referred to in this report as complexes 1a and 1b, while the lower band will be referred to as complex 2. Complex 2, corresponding to H2TF1 as originally identified (6), forms most readily with DNA sequences derived from the MHC class I and $\beta_2$-microglobulin promoters (Fig. 1). In addition, small amounts of complex 2 form with a DNA encoding an NF-κB site located approximately 1,100 bp upstream from the murine c-*myc* transcription start site (Fig. 1). The complex 1 doublet forms most readily with the MHC region I enhancer and $\beta_2$-microglobulin-derived sequences; however, it forms with other NF-κB sites, including those found in the Ig κ and c-*myc* enhancers and in the HIV long terminal repeat (Fig. 1). An imperfect repeat of the MHC RI sequence (MHC RIIa) is found 4 bases upstream of MHC RI, stretching from −177 to −189 (Table 1). This site forms only complex 1b when tested against the HeLa B extract (Fig. 1). A mutant of the MHC RI site with a double point mutation is incapable of forming DNA-protein complexes, illustrating the specificity of interactions with other members of the panel (Fig. 1). Thus, H2TF1 complex 2 binds to a subset of NF-κB sites, while complexes 1a and 1b are formed in the presence of virtually all NF-κB sites tested.

**Identification of a DNA-binding subunit of H2TF1 by DNA cross-linking.** We then designed a probe (UV21) corresponding to the *H-2K*$^b$ region I enhancer and used a UV cross-linking protocol to determine the size(s) of the DNA-binding component(s) of H2TF1 (17). When used in a mobility shift assay with the HeLa B fraction, the UV21 probe generated a pattern of DNA-protein complexes similar to that shown in Fig. 1, lane 1 (data not shown). HeLa B-UV21 binding reactions were UV cross-linked for increasing lengths of time and analyzed by SDS-PAGE. Under these conditions, a major cross-linked protein doublet was observed with a mobility corresponding to approximately 125 kDa (Fig. 2A, lanes 1 to 4). The efficiency of the cross-linking reaction was seen to be directly proportional to the length of time that the reaction mix was UV irradiated. Proteinase K treatment destroys the cross-linked complex, establishing the DNA-binding component as a protein (Fig. 2A, lane 5). When UV irradiation was omitted, no complex was formed (data not shown).

The specificity of this interaction was explored by adding DNA competitors during the binding reaction. Competition with a 10-fold excess of unlabeled UV21 DNA markedly decreased binding, while a 10-fold excess of a DNA containing a mutated H2TF1 binding site (UV23) had little effect on the lower member of the doublet (Fig. 2A, lanes 6 and 7). In addition, no protein-DNA complexes in the 125-kDa range were detected when labeled UV23 was used in a binding reaction (Fig. 2A, lane 8). As will be shown below, cross-linked NF-κB subunits form much smaller complexes. Thus, while H2TF1 shares binding sites with NF-κB, it contains a DNA-binding subunit of a size quite different from that described for NF-κB and c-Rel.

**Subcellular localization of H2TF1.** Given the similarities in DNA-binding specificity between NF-κB and H2TF1 and the cytoplasmic localization of inactive NF-κB, we were interested in determining the subcellular localization of H2TF1. We prepared nuclear and cytoplasmic extracts as described in Materials and Methods, taking care to avoid cytoplasmic contamination by spinning nuclei over a sucrose pad. Under these conditions, virtually all the H2TF1 DNA-binding activity was found in cytoplasmic extracts, with only trace amounts of DNA-binding activity in nuclear extracts (Fig. 2B, lanes 1 and 2). Interestingly, deoxycholate dissociation was not required to observe cytoplasmic H2TF1 DNA-binding activity (6). Figure 2B (lanes 1 and 2) identifies three cytoplasmic complexes as C1 through C3 and two nuclear complexes as N1 and N2. In order to determine the size of the DNA-binding components of these complexes, solution cross-linked material was separated by EMSA, excised from the native gel shown in Fig. 2 (lanes 1 and 2), equilibrated with SDS-PAGE loading buffer, and placed into the wells of an SDS-PAGE gel. As shown in Fig. 2B, complexes C1 and C2 (lanes 3 and 4) both contain a protein which, upon

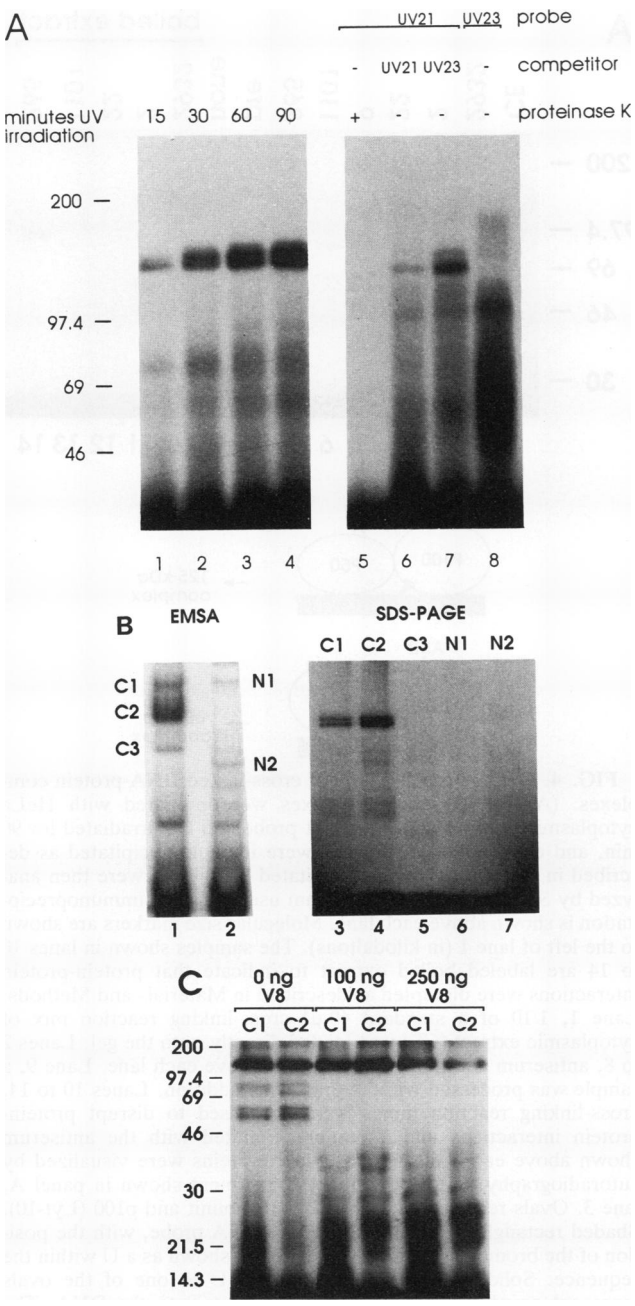


FIG. 2. Covalent cross-linking of DNA-binding subunits of H2TF1 to a DNA probe. (A) The UV21 probe was incubated with a HeLa whole-cell extract and exposed to 302-nm UV irradiation. Lanes 1 to 4 correspond to 15, 30, 60, and 90 min of UV irradiation, respectively. The samples were then subjected to SDS-PAGE and visualized by autoradiography. Samples shown in lanes 5 to 8 were UV irradiated for 90 min and analyzed by SDS-PAGE. In lane 5, the binding reaction mix was incubated with proteinase K for 30 min after cross-linking. In lane 6, the UV21 probe was incubated with extract in the presence of a 10-fold excess of unlabeled competitor UV21 DNA prior to cross-linking. In lane 7, the UV21 probe was incubated with extract in the presence of a 10-fold excess of unlabeled competitor UV23 mutant DNA prior to cross-linking. In lane 8, extract was cross-linked to the UV23 mutant DNA probe. (B) Binding reaction mixes were UV irradiated for 90 min and then subjected to native gel electrophoresis (EMSA). Gel slices containing shifted DNA-protein complexes were excised after autoradiography, equilibrated with SDS loading buffer, and analyzed by SDS-PAGE. Lanes 1 and 2, EMSA of nuclear and cytoplasmic binding reactions, respectively. Shifted complexes are identified as C1 through C3 (lane 1) and N1 and N2 (lane 2). The band at the bottom of lanes 1 and 2 represents free probe. Lanes 3 to 7, excised gel slices containing the bands identified in lanes 1 and 2 which were analyzed by SDS-PAGE. The excised complex is shown at the top of each lane. (C) Partial proteolysis of the C1 and C2 complexes shown in panel B. Binding reaction mixes containing HeLa cytoplasmic extract were cross-linked in triplicate and separated by mobility shift gel electrophoresis. The appropriate bands were excised, equilibrated with SDS loading buffer, loaded onto a 10% SDS gel, and overlaid with 0, 100, or 250 ng of endoproteinase C (V8) as shown above the lanes. The samples were digested as described in Materials and Methods. Molecular size markers are shown to the left of lane 1 (in kilodaltons).

cross-linking to UV21, migrates at 125 kDa. These major cross-linked complexes derived from the EMSA complexes C1 and C2 migrate identically in SDS-PAGE gels to the solution cross-linked 125-kDa complex of Fig. 2A (data not shown). In comparison, with PhosphorImager cassette exposure times of up to 4 days, we failed to detect this complex in lanes corresponding to C3, N1, or N2. In addition to the major 125-kDa complex observed in C1 and C2, we observed various amounts of faster-migrating complexes, similar to those in Fig. 2A (compare lane 4 in Fig. 2A with lane 4 in Fig. 2B).

The identical mobilities of the cross-linked C1 and C2 complexes suggested that these complexes contained the same DNA-binding subunit. In order to further compare the C1- and C2-derived cross-linked protein complexes, we subjected these complexes to limited proteolytic digestion with endoproteinase Glu-C (V8) during SDS-PAGE. Cytoplasmic extracts were cross-linked to the UV21 probe and separated by mobility shift assay, and the shifted complexes corresponding to C1 and C2 were excised after autoradiography as above. These gel slices were then equilibrated with SDS buffer, loaded into SDS-PAGE wells, overlaid with protease solution, and electrophoresed as described in Materials and Methods. As shown in Fig. 2C, both complexes, upon partial digestion by V8, generated a similar pattern, suggesting that these proteins are highly similar or identical.

**Interaction of the DNA-binding subunit of H2TF1 with antiserum specific for NF-κB/Rel family members.** The strong similarity between the H2TF1 and NF-κB methylation interference patterns and the cytoplasmic localization of both molecules suggested that H2TF1 might have some structural similarities to NF-κB/Rel family members (7). We explored this possibility with a panel of NF-κB and Rel antibodies (see Materials and Methods). When antiserum raised against p50, p65, or c-Rel was incubated with binding reaction mixes containing the HeLa B fraction and analyzed by mobility shift assay, no changes in mobility were observed (Fig. 3, lanes 1 to 5). In comparison, when antiserum raised against p100 (Lyt-10) was added to binding reaction mixes, the C2 complex was shifted to the top of the gel (Fig. 3, lane 6). This interaction is specific in that the peptide against which the p100 antibody was made (p100 peptide) blocked the supershift, while an irrelevant peptide had no effect (Fig. 3, lanes 7 and 8).

As it was difficult to determine whether the p100 antiserum supershifted C1 in the presence of supershifted C2, we repeated the supershift experiment with the Ig κ probe, which shifts only the C1 complexes. While antiserum raised against p50, p65, or c-Rel had little effect (data not shown),

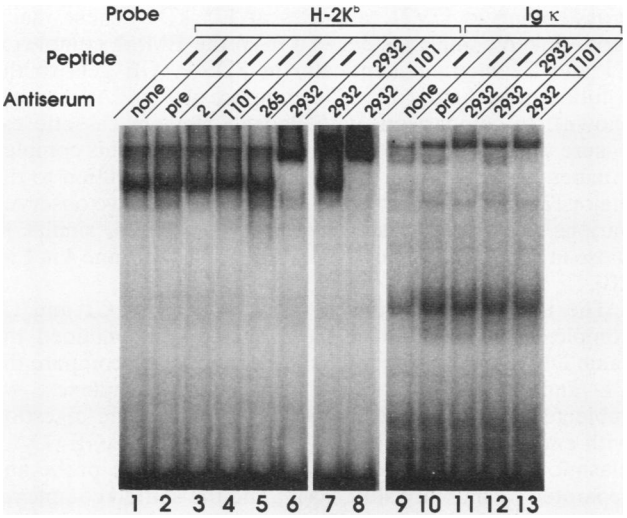


FIG. 3. Interaction of H2TF1 with NF-κB/Rel antiserum in a mobility shift assay. Binding reaction mixes prepared with HeLa cytoplasmic extracts and either the UV21 probe (lanes 1 to 8) or the Ig κ probe (lanes 9 to 13) were allowed to equilibrate for 30 min, after which 1 μl of either preimmune serum or NF-κB/Rel antiserum was added. Where indicated, peptide was added to the binding reaction mixes just before antibody addition. Binding reaction mixes were analyzed by EMSA in TAE gels. The antiserum and/or peptide added to each reaction mix is shown above each lane. The band at the bottom of the gel represents free probe.

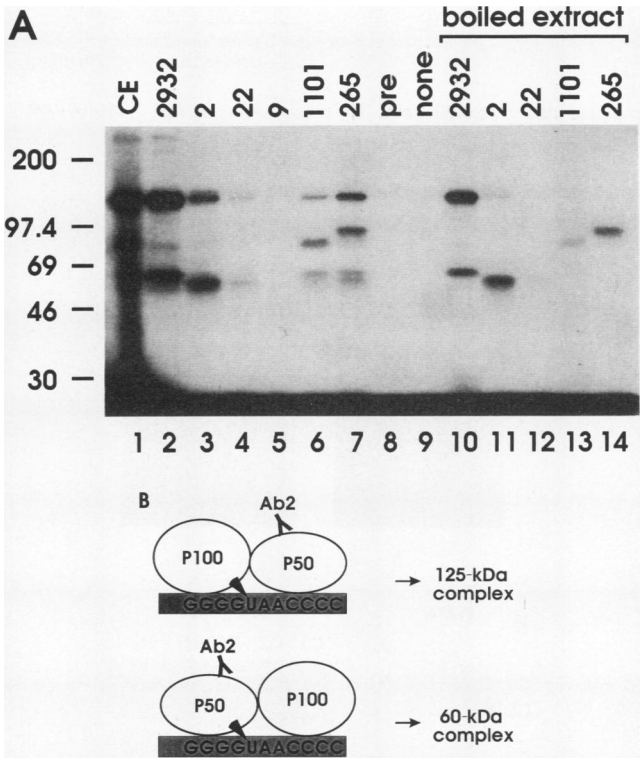


FIG. 4. Immunoprecipitation of cross-linked DNA-protein complexes. (A) Binding reaction mixes were prepared with HeLa cytoplasmic extracts and the UV21 probe and UV irradiated for 90 min, and cross-linked complexes were immunoprecipitated as described in the text. Immunoprecipitated complexes were then analyzed by SDS-PAGE. The antiserum used for each immunoprecipitation is shown above each lane. Molecular size markers are shown to the left of lane 1 (in kilodaltons). The samples shown in lanes 10 to 14 are labeled boiled extract to indicate that protein-protein interactions were disrupted as described in Materials and Methods. Lane 1, 1/10 of a standard 40-μl cross-linking reaction mix of cytoplasmic extract (CE) was loaded directly onto the gel. Lanes 2 to 8, antiserum additions are as shown above each lane. Lane 9, a sample was processed without antiserum addition. Lanes 10 to 14, cross-linking reaction mixes were processed to disrupt protein-protein interactions and immunoprecipitated with the antiserum shown above each lane. Cross-linked proteins were visualized by autoradiography. (B) Model of the experiment shown in panel A, lane 3. Ovals represent the NF-κB p50 subunit and p100 (Lyt-10). Shaded rectangles represent the UV21 DNA probe, with the position of the bromodeoxyuridine substitution shown as a U within the sequence. Solid triangles connecting the U to one of the ovals represent covalent cross-linking of the protein to the DNA. The inverted Y represents antibodies from the Ab2 antiserum and is labeled Ab2. The binding site is palindromic; hence, a dimer can bind in either orientation. This is shown by the lower and upper groups. The expected complex generated from each group is shown to the right of the arrows.

p100 antiserum clearly supershifted the lower C1 complexes (Fig. 3, lane 11). The addition of preimmune serum markedly increased nonspecific DNA binding in the upper region of the C1 complexes, hindering the interpretation of this experiment (Fig. 3, compare lanes 9 and 10). This interaction between p100 antiserum and the C1 complexes could be blocked by p100 peptide but not by an irrelevant peptide (Fig. 3, lanes 12 and 13). Thus, anti-p100 antiserum interacts with some of the C1 EMSA complexes as well as with the C2 complex.

HeLa cell p100 migrates as a 114-kDa protein when analyzed by SDS-PAGE (43). The ability of anti-p100 antiserum to interact with both C1 and C2 and the similarity in size between p100 and the 125-kDa complex strongly suggest that p100 is a component of H2TF1. It is important to note that the lack of interaction between other NF-κB or Rel antibodies and these complexes does not indicate their absence, only our inability to demonstrate their presence in this assay. Indeed, as described below, Rel/NF-κB family members do interact with cytoplasmic p100.

**Physical association of p100 (Lyt-10) with Rel/NF-κB subunits.** To further explore the associative properties of the major DNA-binding component of H2TF1, we covalently labeled κB motif-binding proteins from HeLa extracts by UV cross-linking with the UV21 DNA probe. HeLa cell cytoplasmic extracts, when cross-linked to the UV21 probe and analyzed directly by SDS-PAGE, generate one major DNA protein complex at 125 kDa and several other complexes of 88, 80, 65, and 60 kDa (Fig. 4A, lane 1). As will be shown below, these complexes consist of p100, c-Rel, p65, p52 (a product derived from p100), and p50, respectively. It is useful to consider Fig. 4B when analyzing the data shown in Fig. 4A. The UV21 probe contains a palindromic κB site which is expected to bind dimeric proteins. By design, there is only one bromodeoxyuridine substitution within the binding site; hence, only one member of the dimer can be covalently linked to the probe. As shown by way of example in Fig. 4B, the cross-linking of the probe to the p100 subunit of a putative p100-p50 heterodimer results in a 125-kDa complex when analyzed by SDS-PAGE. Cross-linking of the probe to the p50 subunit, however, results in a 60-kDa cross-linked complex. Consistent with this model, both cross-linked species can be immunoprecipitated by an anti-p50 antibody, as shown in Fig. 4A, lane 3.

When cross-linked extract is incubated with anti-p100 antiserum, all of the above complexes are coimmunoprecipitated, but the precipitate is enriched in the 125-kDa (p100) and 65-kDa (p52) species (Fig. 4A, lane 2). When one of several antisera raised against p50 is substituted, the 60-kDa (p50) species is precipitated predominantly, along with the 125-kDa (p100) species (Fig. 4A, lanes 3 and 4). In addition, a polyclonal antiserum raised against p50 (Ab2), which recognizes both homodimeric and heterodimeric p50, immunoprecipitates a trace of the 80-kDa (p65) species (Fig. 4A, lane 3), while an antipeptide antiserum (Ab22) characterized as binding preferentially to p50 homodimers does not immunoprecipitate this species (Fig. 4A, lane 4). An antibody specific for IκBα/MAD-3 does not coimmunoprecipitate any of the DNA-bound complexes (Fig. 4A, lane 5). An antipeptide antiserum raised against p65 immunoprecipitates primarily the 80-kDa (p65) species but also brings down p100, p52, and a trace of p50 (Fig. 4A, lane 6). Finally, an antipeptide antiserum raised against c-Rel primarily immunoprecipitates the 88-kDa (c-Rel) species but also brings down p100 and a trace of p52, p50, and p65 (Fig. 4A, lane 7). In lanes 3, 6, and 7 of Fig. 4A, small amounts of cross-linked p50, p52, and p65, respectively, were detected. Under these UV cross-linking conditions, we may be cross-linking a small amount of IκB-associated proteins. Alternatively, these might represent a small population of multimeric complexes. These possibilities are explored more fully in the Discussion.

The above interpretive description of the data requires that we discriminate between immunoprecipitations through direct antibody contact and those through protein-dimer interactions. To this end, extracts were boiled in 1% SDS after cross-linking to the UV21 probe and diluted to 0.1% SDS as described in Materials and Methods. Under these conditions, anti-p100 immunoprecipitates only the 125-kDa (p100) and 65-kDa (p52) species (Fig. 4A, lane 10). Interestingly, while Ab2 immunoprecipitated primarily the 60-kDa (p50) species, a trace of the 125-kDa (p100) species was still brought down (Fig. 4A, lane 11). Ab22 immunoprecipitated only the 60-kDa (p50) species (Fig. 4A, lane 12). Finally, the anti-p65 and anti-c-Rel antisera immunoprecipitated only the 80-kDa (p65) and 88-kDa (c-Rel) species, respectively (Fig. 4A, lanes 13 and 14). We then extended these observations by performing an identical experiment with HeLa cell nuclear extract. We found no detectable p100 or p52 and only trace amounts of p50 or p65 cross-linked to the UV21 probe (data not shown). These data are most simply explained as showing direct physical interaction of cytoplasmic p100 and p52 with other Rel family members.

In order to determine whether the 125-kDa complex immunoprecipitated from boiled extract by Ab2 (Fig. 4A, lane 11) is p100 or perhaps p105, κB-binding proteins from the HeLa cell cytoplasmic extract were cross-linked to the UV21 probe and incubated with an excess of Ab2932 (anti-p100 antiserum). After removing all Ab2932-binding proteins by incubation with PAS, the supernatant, cleared of p100, was incubated with Ab2. Under these conditions, we were able to immunoprecipitate small amounts of the 60-kDa species (p50) but not of the 125-kDa species (data not shown). From this result, we conclude that the 125-kDa band in Fig. 4A, lane 11, is cross-linked p100 and either that the p50-p100 interaction is stable enough that a small portion reforms after boiling or that the polyclonal Ab2 is able to recognize some minor epitopes present in p100. The large decrease in the presence of the 125-kDa species after boiling of the extract suggests that p100 is immunoprecipitated by

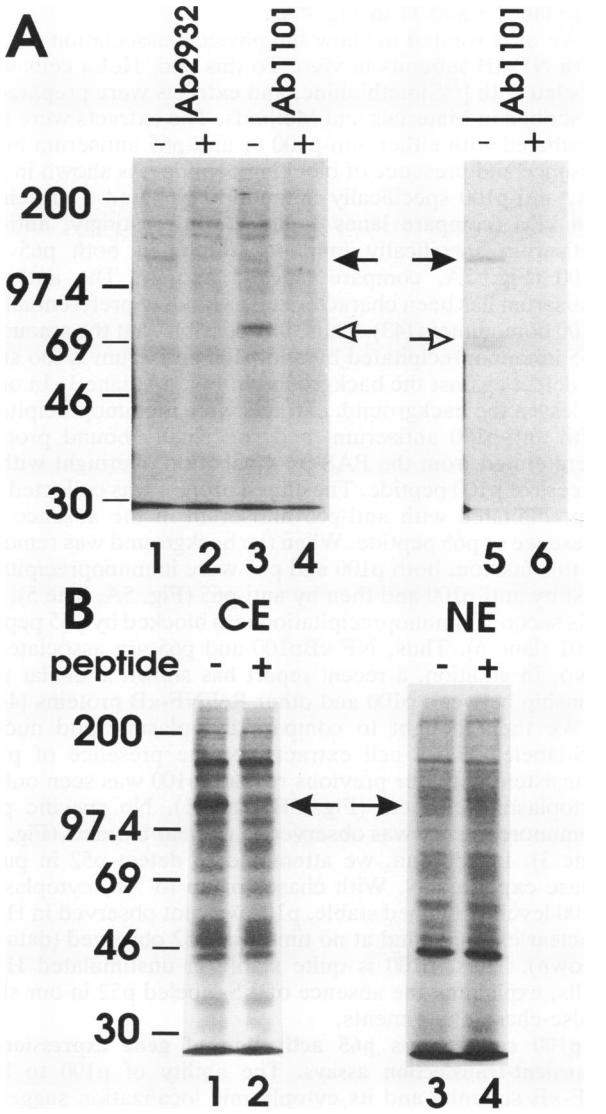


FIG. 5. Immunoprecipitation of p100 and associated proteins from $^{35}$S-labeled HeLa cell extracts. (A) HeLa cells were labeled with [$^{35}$S]methionine and [$^{35}$S]cysteine as described in the text, and labeled extracts were immunoprecipitated with anti-p100 antiserum Ab2932 (lanes 1 and 2) or with anti-p65 antiserum Ab1101 (lanes 3 and 4). Immunoprecipitations were performed in the absence (−) or presence (+) of excess peptide against which the antibody was made, as shown above each lane. Extract immunoprecipitated with anti-p100 antiserum was eluted from the PAS pellet as described in Materials and Methods and reprecipitated with anti-p65 antiserum in the absence (−) or presence (+) of p65 peptide (lanes 5 and 6). Immunoprecipitated proteins were analyzed by SDS-PAGE and visualized by fluorography. Molecular size markers are shown to the left of lane 1 (in kilodaltons). (B) HeLa cells were labeled with [$^{35}$S]methionine and [$^{35}$S]cysteine and divided into cytoplasmic (CE) and nuclear (NE) extracts as described in Materials and Methods. Immunoprecipitations were performed from cytoplasmic extracts (lanes 1 and 2) and from nuclear extracts (lanes 3 and 4) with anti-p100 antiserum in the absence (lanes 1 and 3) or presence (lanes 2 and 4) of competing p100 peptide, as shown above each lane. Immunoprecipitated proteins were analyzed by SDS-PAGE and visualized by fluorography. Molecular size markers are shown to the left of lane 1. Solid arrows represent p100; open arrows represent p65.

Ab2 primarily through physical interaction with p50 (compare lanes 3 and 11 in Fig. 4A).

We next wanted to show the physical association of p100 with NF-κB subunits in vivo. To this end, HeLa cells were labeled with [$^{35}$S]methionine, and extracts were prepared as described in Materials and Methods. The extracts were then incubated with either anti-p100 or anti-p65 antiserum in the absence and presence of blocking peptide. As shown in Fig. 5A, anti-p100 specifically immunoprecipitated a protein of 114 kDa (compare lanes 1 and 2). Interestingly, anti-p65 antiserum specifically immunoprecipitated both p65 and p100 (Fig. 5A, compare lanes 3 and 4). The anti-p100 antiserum has been characterized as binding preferentially to p100 homodimers (43). Thus, it is possible that the amount of p65 immunoprecipitated by anti-p100 antiserum is too small to detect against the background in Fig. 5A, lane 1. In order to lessen the background, extracts were immunoprecipitated with anti-p100 antiserum, and specifically bound proteins were eluted from the PAS by incubation overnight with an excess of p100 peptide. The eluted protein was collected and reprecipitated with anti-p65 antiserum in the absence and presence of p65 peptide. When the background was removed in this fashion, both p100 and p65 were immunoprecipitated first by anti-p100 and then by anti-p65 (Fig. 5A, lane 5), and this second immunoprecipitation was blocked by p65 peptide 1101 (lane 6). Thus, NF-κBp100 and p65 are associated in vivo. In addition, a recent report has shown a similar relationship between p100 and other Rel/NF-κB proteins (44).

We then thought to compare cytoplasmic and nuclear $^{35}$S-labeled HeLa cell extracts for the presence of p100. Consistent with our previous results, p100 was seen only in cytoplasmic extracts (Fig. 5B, lane 1). No specific p100 immunoreactivity was observed in nuclear extracts (Fig. 5B, lane 3). In addition, we attempted to detect p52 in pulse-chase experiments. With chases of up to 7 h, cytoplasmic p100 levels remained stable, p100 was not observed in HeLa nuclear extracts, and at no time was p52 observed (data not shown). Thus, p100 is quite stable in unstimulated HeLa cells, explaining the absence of $^{35}$S-labeled p52 in our short pulse-chase experiments.

**p100 can repress p65 activation of gene expression in transient-transfection assays.** The ability of p100 to bind NF-κB subunits and its cytoplasmic localization suggested to us that it functions as an IκB-like molecule. We tested this hypothesis by determining whether p65 transcriptional activity could be repressed by p100 in transient-transfection assays. p65 was transfected in the presence of either p100 or the parent vector and tested for its ability to stimulate transcription of a reporter containing three copies of the *H-2K$^b$* κB binding site fused upstream of minimal *fos* promoter linked to the CAT gene (MHC-CAT). As shown in Fig. 6, 200 ng of p65 expression plasmid induces a sixfold activation of the reporter. Cotransfection of equivalent (microgram) amounts of p65 and the p100 expression plasmid resulted in a 40 to 50% reduction in CAT activity. When the amount of p100 DNA was increased fivefold (corresponding to a 4.3-fold molar excess of p100 plasmid), we saw a complete repression of p65 stimulation of the reporter. In comparison, IκB, when transfected in equal (microgram) amounts, can inhibit p65 to within 10% of basal expression (9); however, it is difficult to know the relative efficiencies of translation of the two plasmids or the stability of their products. When the p65 DNA amount was then increased fivefold, so that p100 and p65 expression plasmids were again present in equal amounts, p65 activation was partially restored. Transfection of p100 alone had no effect on MHC-CAT expression. Thus, the effects of p100 on p65 are titratable and depend on the ratio of p65 to p100.

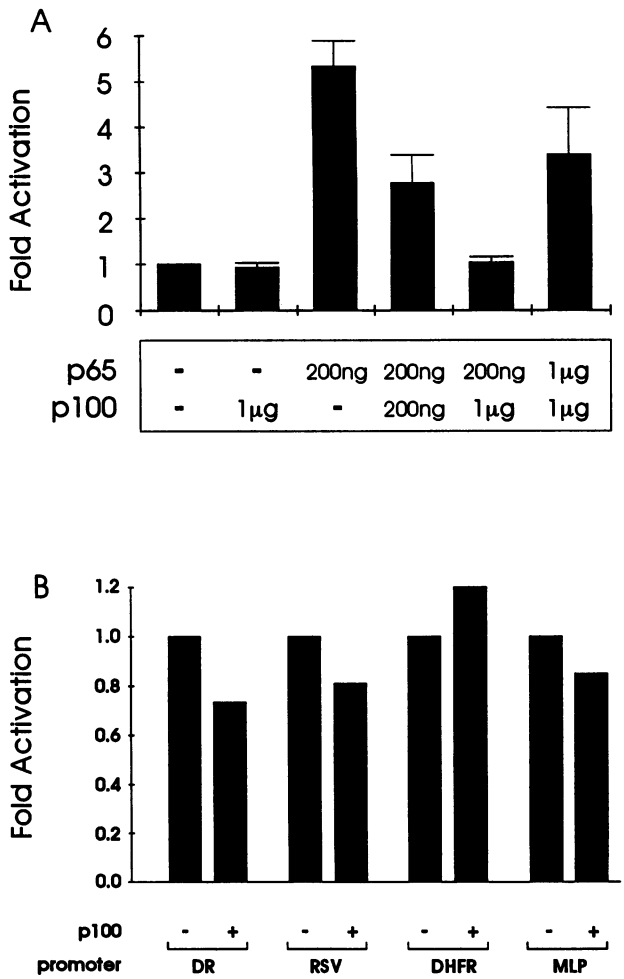


FIG. 6. p100 represses p65 activation in transient-transfection assays. For each condition tested, 5 × 10$^6$ HeLa cells were transfected by electroporation. Transfected cells were grown for 16 h and then harvested. Extracts were assayed for CAT activity and protein concentration. (A) Each transfection mix contained 20 μg of DNA with a constant molar amount of cytomegalovirus (CMV) promoter DNA, 5 μg of the MHC3×CAT reporter, and various amounts of CMV-p65 and CMV-p100 expression plasmids, as shown below the graph. The data were normalized to input protein levels and are expressed as fold activation above basal reporter activity, representing three separate measurements from at least two different preparations of p65 and p100 expression plasmids. (B) Each transfection mix contained 20 μg of DNA with a constant molar amount of CMV promoter DNA and 5 μg of reporter plasmid. Each reporter plasmid was transfected in the presence or absence of 1 μg of the CMV-p100 expression plasmid. The data were normalized as for panel A. The basal CAT activity of each reporter alone is assigned a value of 1. Reporter activity in the presence of 1 μg of CMV-p100 expression plasmid is expressed as fold activation over basal activity. Promoters are as follows: RSV, Rous sarcoma virus; DR, MHC class II DR element; DHFR, dihydrofolate reductase promoter; MLP, adenovirus major late promoter.

By immunoblotting, we found that cotransfected p100 had no effect on the level of transfected p65 expression (data not shown). Interestingly, transfected p100 protein could be detected in the nucleus, suggesting that the ankyrin repeats alone are not sufficient to block nuclear transport. We also

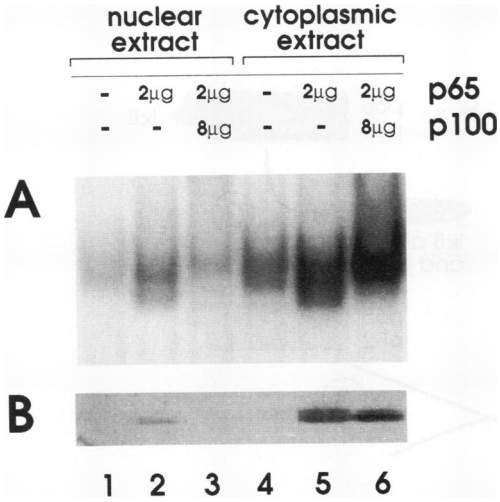


FIG. 7. Transfected p100 sequesters p65 in the cytoplasm. COS cells were transfected by DEAE-dextran with 10 μg of DNA consisting of a constant molar amount of CMV vector DNA and various amounts of CMV-p65 and CMV-p100 expression plasmids. After 48 h, nuclear and cytoplasmic extracts were prepared. Lanes 1 to 3, nuclear extracts; lanes 4 to 6, matched cytoplasmic extracts. Lanes 1 and 4, COS cells transfected with the CMV vector alone; lanes 2 and 5, COS cells transfected with 2 μg of CMV-p65; lanes 3 and 6, COS cells transfected with 2 μg of CMV-p65 plus 8 μg of CMV-p100. (A) Binding reactions of deoxycholate-treated extracts with the UV21 DNA probe analyzed by EMSA. Only the shifted bands are shown. (B) Immunoblot analysis of COS extracts (matched to those in panel A) with the p65-specific antiserum 1101.

tested the specificity of p100-mediated repression by replacing the κB reporter with reporters unresponsive to p65, including the adenovirus major late promoter (MLP-CAT), the Rous sarcoma virus promoter (RSV-CAT), the MHC class II DR promoter (DR-CAT), and the dihydrofolate reductase promoter (DHFR-CAT). As shown in Fig. 6B, p100 had negligible effects on the activity of these promoters, suggesting that its effects are specific to p65 stimulation rather than to basal expression. In addition, the repression of p65 activation by p100 was observed in Jurkat and COS cells and also in HeLa cells with a reporter driven by the HIV long terminal repeat (data not shown).

**Transfected p100 sequesters p65 in the cytoplasm.** In order to better understand the mechanism by which p100 repressed p65 activation, we analyzed matched nuclear and cytoplasmic extracts derived from transfected COS cells by both EMSA and immunoblotting. COS cells were chosen because our antiserum is specific for human NF-κB subunits, allowing us to monitor transfected cells. Deoxycholate-treated nuclear and cytoplasmic extracts derived from COS cells transfected with vector alone contain relatively little NF-κB binding activity, as measured by EMSA (Fig. 7A, lanes 1 and 4). Transfection of p65 resulted in an increase in DNA-binding activity which was observed in both nuclear and cytoplasmic extracts (Fig. 7A, lanes 2 and 5). When a fourfold excess of p100 expression plasmid was cotransfected, nuclear DNA-binding activity was strongly decreased and cytoplasmic DNA-binding activity was increased and shifted to a slightly slower-migrating complex (Fig. 7A, lanes 3 and 6). This might indicate that p100 competes with nuclear p65 for DNA binding or that, through heterodimerization, p100 blocks p65 from entering the nucleus.

In order to discriminate between these possibilities, we analyzed these extracts for p65 immunoreactivity by immunoblotting with Ab1101. p65 immunoreactivity was only observed in p65-transfected cells (Fig. 7B) and was blocked by mixing Ab1101 with the peptide from which it was generated (data not shown). Transfection with p65 results in the appearance of both nuclear p65 protein and a large pool of cytoplasmic p65 (Fig. 7B, lanes 2 and 5). This cytoplasmic pool is likely formed by the p65-mediated induction of IκBα (14, 63). It is thought that the induction of IκBα ensures that physiological stimulation of NF-κB results in a transient pulse of NF-κB activity. Cotransfection of p65 with p100 results in the loss of nuclear p65 protein and an increase in cytoplasmic p65 protein levels (Fig. 7B, lanes 3 and 6). Thus, while p100 may compete with p65 for DNA binding, it clearly sequesters p65 in the cytoplasm and, in doing so, satisfies the functional requirements for membership in the IκB family of NF-κB regulators.

## DISCUSSION

**NF-κB precursors function as IκB-like molecules.** The data presented above have shown by several experimental methods that NF-κB p100 is a DNA-binding component of H2TF1 and that NF-κB p100 is bound to NF-κB subunits in the cytoplasm. As transfected p100 sequesters p65 in the cytoplasm and represses p65 activation, we interpret its cytoplasmic role as an IκB-like regulator of NF-κB activity. Among the members of the *rel* multigene family, p100 shows the greatest similarities with p105. This suggests that p105 might also have p100's IκB-like function. While this article was in preparation, just such an observation was published by several groups (16, 46, 53). Thus, these studies, with ours and that of Mercurio et al. (44), together demonstrate a new mechanism, general to NF-κB precursor molecules, by which NF-κB activity is regulated.

The NF-κB precursor molecules p100 and p105 contain ankyrin repeat domains homologous with those found within the IκB family (49, 51, 56). Deletion studies have shown that these repeat structures play a role in the inhibition of DNA binding (27, 31, 40, 65). Interestingly, different members of the IκB family have different affinities for NF-κB dimers. IκBα and pp40 bind preferentially to p65 and poorly to p50 (9), while Bcl-3 binds specifically to p50 (65) and p52 (11). The C-terminal region of p105, when expressed separately, binds preferentially to p50 (40); however, p105, like p100, has been shown to associate with c-Rel and p65 as well (53). This suggests that the activities of different NF-κB/Rel complexes are regulated independently by selective activation through different IκB family members. Surprisingly, p52/Bcl-3 complexes have recently been shown to activate gene transcription through κB binding sites (11), indicating that the role of ankyrin domain-containing proteins as NF-κB regulators is complex.

The similarities between p105 and p100 caused researchers to look for and find an N-terminally processed form, p52, which has been shown to synergize with p65 to activate transcription through NF-κB sites (43, 52, 55). Therefore, the processing of p100-Rel family heterodimers to p52-Rel family heterodimers allows both regulated expression of the transcription factors and the combinatorial specificity that is presumably associated with the control of gene expression through various κB-like elements. An identical argument can be made for p105-Rel family heterodimers as well. Indeed, others have shown by pulse-chase experiments that cytoplasmic p105-Rel heterodimers give rise to nuclear p50-Rel

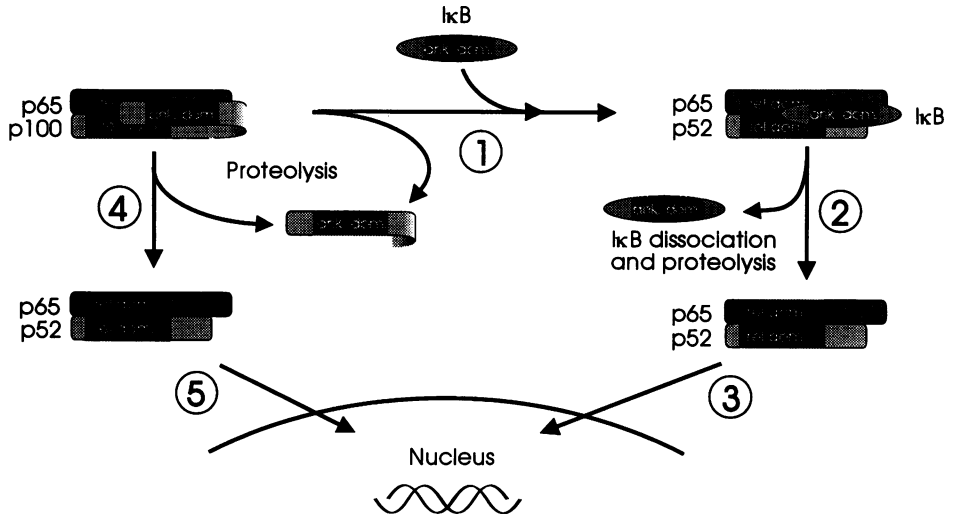


FIG. 8. Model of the regulation of NF-κB precursors. Shaded rectangles represent p65, p100, and p52 and are identified to the left of each rectangle. IκB is represented by a shaded oval. The Rel homology domain (rel dom.) and ankyrin repeat domain (ank. dom.) of each protein are shown as darker shaded rectangles. The ankyrin repeat domain of p100 is shown folded over the C-terminal portion of the Rel homology domains of p65 and p100 to indicate masking of the nuclear localization signal, in a manner similar to that of IκB. Proteolytic processing of precursor heterodimers, IκB dissociation, and nuclear translocation of p52-p65 complexes are shown as separate steps and labeled 1 through 5. The C-terminal portion of p100 removed by proteolysis is shown in steps 1 and 4. These steps are discussed further in the text.

heterodimers upon phorbol myristate acetate stimulation (44, 53).

Little is known of the mechanisms by which stimuli activate NF-κB. In vitro studies have shown that phosphorylation of IκB blocks its ability to bind NF-κB, suggesting that activation of a kinase is a step in the transactivation pathway (22). Consistent with this model, we have recently detected a phosphorylated form of IκBα following treatment with tumor necrosis factor alpha or interleukin-1. Certain stimuli, such as tumor necrosis factor alpha, however, have been shown to activate NF-κB through a pathway independent of protein kinases A and C (29, 42), which might involve the production of oxygen radicals (57, 61). Equally little is known of the mechanism by which proteolytic processing of NF-κB precursors is regulated other than that it is an ATP-dependent process (20).

The discovery that NF-κB precursors themselves sequester Rel family members in the cytoplasm suggests that the mechanisms of NF-κB activation are more complicated than previously thought. Figure 8 summarizes our thoughts as to how cytoplasmic precursor complexes might fit in with the classic model of NF-κB activation. It should be noted that this model is an extension of the data presented here and represents a working hypothesis to be tested by future experiments. The beginning complex is shown as a representative p100-p65 heterodimer; however, one could substitute p105 for p100 and p50, p52, or c-Rel for p65. In step 1, proteolytically cleaved precursor complexes are bound by newly synthesized IκB molecules, forming a cytoplasmic pool of inactive NF-κB/IκB complexes. The processing of these heterodimeric precursor complexes is probably one of several pathways leading to a cytoplasmic pool of NF-κB/IκB complexes. Steps 2 and 3 represent the classic NF-κB/IκB activation pathway (see references 8, 14, and 63). Some processed complexes might escape association with IκB and follow step 4, resulting in a low basal level of NF-κB-like activity. Interestingly, if the rate of proteolytic processing of NF-κB precursor complexes is increased (due to some physiological signal), the production of functional NF-κB-like molecules may initially outpace the constitutive synthesis of IκB, thus favoring step 4 over step 1. Under these conditions, rapid activation of processing could constitute a new mechanism of induction of NF-κB activity. To date, the evidence supports a slow induction of precursor processing (44, 53); however, future experiments may identify a stimulus which mediates a more rapid induction of precursor processing. Thus, the fate of precursor complexes apparently rests on the relative rates of IκB synthesis and precursor processing.

In Fig. 4, lanes 6 and 7, we detected small amounts of cross-linked p50 and p52 immunoprecipitated from HeLa cell cytoplasmic extracts by anti-p65 and anti-c-Rel antibodies. How is it possible for cytoplasmic p50 to associate with p65 without being bound by IκB? While the model shows the precursors p100 and p105 binding to NF-κB subunits as heterodimers, we cannot discount the possibility that multimeric complexes exist as well. Indeed, in reticuloendotheliosis virus T-infected cells, the multimeric v-Rel-containing cytoplasmic complex contains p105 (16). These data can also be explained, however, by the ability of DNA under energetic UV cross-linking conditions to compete (albeit with low affinity) with IκB for p50 binding. In this manner, UV irradiation may trap a small portion of IκB-associated proteins, covalently linking them to DNA.

**Characterization of H2TF1, a cytoplasmic DNA-binding protein complex, as containing p100.** We began this study by analyzing the DNA-binding activity known as H2TF1. Our data demonstrate that a major component of H2TF1 DNA-binding activity is p100 (Lyt-10). Cross-linking experiments (Fig. 2B and C) demonstrate that H2TF1 (the C2 complex in gel shift assays) contains p100 as well as c-Rel, p65, p52, and p50; however, these are not all associated in the same complexes (Fig. 4A). Similarly, the C1 complex contains p100 and might contain other Rel family members. The reason for its slower mobility in gel shift assays is unknown, but it may represent as yet unidentified proteins associated

with this cytoplasmic complex. The data presented here suggest that the H2TF1 DNA-binding activity represents a collection of p100-Rel family member heterodimers (and possibly multimers). Further molecular analysis of these complexes will most likely reveal a diverse set of independent roles rather than one concerted role for H2TF1.

Both p105 and p100 have been shown to bind poorly to DNA in vitro (35, 47). Earlier studies characterizing these precursor molecules as being unable to bind DNA were performed on in vitro-translated or bacterially purified material, whereas this study has characterized an in vivo form of p100. One interpretation for the ability of endogenous H2TF1 to bind DNA effectively is that p100 is modified by a posttranslational modification not present in p100 generated in vitro. p100 might effectively bind DNA only when in a heterodimeric or multimeric configuration. Alternatively, a posttranslational modification of p100 might expose or stabilize the DNA-binding domain. Another possibility is that bacterially expressed or in vitro-translated p100 is not properly folded for efficient binding to DNA, in contrast to H2TF1. We have recently shown that IκB sequesters NF-κB in the cytoplasm by masking the nuclear localization signal (9). This association functions to block the ability of NF-κB p65 to bind to DNA. Here we show that an ankyrin repeat-containing protein, p100 (Lyt-10), is presumably capable of masking the nuclear localization signal without blocking the ability of H2TF1 or the detected p100-Rel protein heterodimers to bind to DNA. In this regard, the Rel domain and the ankyrin repeat-containing domain of p100 may be unique.

The observation that H2TF1 can bind DNA raises the intriguing possibility that if it can enter the nucleus, it could participate directly in the regulation of transcription through κB sites. In this regard, the preference of some forms of H2TF1 for the MHC class I and $\beta_2$-microglobulin κB sites (see Fig. 1) suggests that its role might involve regulation of the expression of proteins involved in antigen presentation.

Mapping of the human p105 and p100 genes has revealed them to be located within loci associated with translocations in certain leukemias (41). Indeed, p100 was cloned as Lyt-10 from just such a translocation (47). The resultant chimera retains the Rel homology domain but has lost the C-terminal ankyrin repeats and can bind DNA as readily as in vitro-generated p100. As we have shown that endogenous p100 can bind DNA, we suspect that the oncogenic potential of the chimera is due either to the loss of cytoplasmic localization engineered by the loss of the ankyrin repeat domain or to an alteration in the chimera's binding specificity.

In summary, we have presented evidence for a mechanism by which NF-κB activity is regulated through associations with the ankyrin repeat-containing precursor protein p100 (Lyt-10). Furthermore, these associations expand the potential for regulation through various κB sites by expanding the combinatorial potential associated with these proteins. The potential importance of this mechanism is illustrated by the dysregulation of the p100 gene resulting from certain translocations in B-cell lymphomas. Future experiments will be aimed at understanding the molecular mechanisms controlling the processing of the NF-κB precursors and identifying potentially new κB-like sites that respond to the relative complexity of Rel family heterodimers. These issues are crucial to the understanding of both NF-κB physiology and the role of NF-κB/Rel members in the development of cancer.

## ACKNOWLEDGMENTS

We thank D. Potter, P. Sharp, J. DiDonato, F. Mercurio, M. Karin, R. Schmid, and G. Nabel for helpful discussions and the generous sharing of data prior to publication. We also thank N. Rice, A. Israel, and members of the Karin laboratory for their gifts of antisera and peptides. In addition, we thank R. Schmid and G. Nabel for the p100 plasmid.

This research was supported by grants from the National Institute of Health to A.S.B. (CA 52515), a March of Dimes Basil O'Conner research award, an R. J. Reynolds-Nabisco scholar award in Immunology, and an American Cancer Society junior faculty research award (JFRA-309). R.I.S. was supported by a fellowship from the Arthritis Foundation.

## ADDENDUM IN PROOF

An amino acid sequence derived from purified H2TF1 has been shown to be identical to NF-κB p100 (D. Potter, C. Larson, P. Eckes, R. Schmid, G. Nabel, G. Verdine, and P. Sharp, J. Biol. Chem., in press).

## REFERENCES

1. **Baeuerle, P. A., and D. Baltimore.** 1988. Activation of DNA-binding activity in an apparently cytoplasmic precursor of the NF-κB transcription factor. Cell **53**:211–217.
2. **Baeuerle, P. A., and D. Baltimore.** 1988. IκB: a specific inhibitor of the NF-κB transcription factor. Science **242**:540–546.
3. **Baeuerle, P. A., and D. Baltimore.** 1989. A 65-kD subunit of active NF-κB is required for inhibition of NF-κB by IκB. Genes Dev. **3**:1689–1698.
4. **Baeuerle, P. A., and D. Baltimore.** 1991. The physiology of the NF-κB transcription factor. Hormonal control regulation of gene transcription. Mol. Aspects Cell. Regul. **6**:409–432.
5. **Baldwin, A. S., Jr., J. C. Azizkhan, D. E. Jensen, A. A. Beg, and L. R. Coodly.** 1991. Induction of NF-κB DNA-binding activity during the $G_0$-to-$G_1$ transition in mouse fibroblasts. Mol. Cell. Biol. **11**:4943–4951.
6. **Baldwin, A. S., Jr., and P. A. Sharp.** 1987. Binding of a nuclear factor to a regulatory sequence in the promoter of the mouse *H-2K*$^b$ class I major histocompatibility gene. Mol. Cell. Biol. **7**:305–313.
7. **Baldwin, A. S., Jr., and P. A. Sharp.** 1988. Two transcription factors, NF-κB and H2TF1, interact with a single regulatory sequence in the class I major histocompatibility complex promoter. Proc. Natl. Acad. Sci. USA **85**:723–727.
8. **Beg, A. A., T. S. Finco, P. V. Nantermet, and A. S. Baldwin, Jr.** 1993. Tumor necrosis factor and interleukin-1 lead to phosphorylation and loss of IκB: a mechanism for NF-κB activation. Mol. Cell. Biol. **13**:3301–3310.
9. **Beg, A. A., S. M. Ruben, R. I. Scheinman, S. Haskill, C. A. Rosen, and A. S. Baldwin, Jr.** 1992. IκB interacts with the nuclear localization sequences of the subunits of NF-κB: a mechanism for cytoplasmic retention. Genes Dev. **6**:1899–1913.
10. **Bours, V., P. R. Burd, K. Brown, J. Villalobos, S. Park, R. P. Ryseck, R. Bravo, K. Kelly, and U. Siebenlist.** 1992. A novel mitogen-inducible gene product related to p50/p105-NF-κB participates in transactivation through a κB site. Mol. Cell. Biol. **12**:685–695.
11. **Bours, V., G. Franzoso, V. Azarenko, S. Park, K. Tomohiko, K. Brown, and U. Siebenlist.** 1993. The oncoprotein Bcl-3 directly transactivates through κB motifs via association with DNA-binding p50B homodimers. Cell **72**:729–739.
12. **Bours, V., J. Villalobos, P. R. Burd, K. Kelly, and U. Siebenlist.** 1990. Cloning of a mitogen-inducible gene encoding a κB DNA-binding protein with homology to the rel oncogene and to cell-cycle motifs. Nature (London) **348**:76–80.
13. **Bradford, M. M.** 1976. A rapid and sensitive method for the quantitation of microgram quantities of protein utilizing the principle of protein-dye binding. Anal. Biochem. **72**:248–254.
14. **Brown, K., S. Park, T. Kanno, G. Franzoso, and U. Siebenlist.** 1993. Mutual regulation of the transcriptional activator NF-κB

and its inhibitor, IκBα. Proc. Natl. Acad. Sci. USA **90**:2532–2536.

15. **Brownell, E., N. Mittereder, and N. R. Rice.** 1989. A human rel proto-oncogene cDNA containing an Alu fragment as a potential coding exon. Oncogene **4**:935–942.
16. **Capobianco, A. J., D. Chang, G. Mosialos, and T. D. Gilmore.** 1992. p105, the NF-κB p50 precursor protein, is one of the cellular proteins complexed with the v-Rel oncoprotein in transformed chicken spleen cells. J. Virol. **66**:3758–3767.
17. **Chodosh, L. A.** 1989. Crosslinking of proteins to nucleic acids, p. 12.5.1–12.5.3. *In* F. M. Ausubel, R. E. Brent, D. D. Kingston, J. G. Moore, J. G. Seidman, J. A. Smith, and K. Struhl (ed.), Current protocols in molecular biology. John Wiley & Sons, New York.
18. **Cleveland, D. W.** 1983. Peptide mapping in one dimension by limited proteolysis of sodium dodecyl sulfate-solubilized proteins. Methods Enzymol. **96**:222–229.
19. **Davis, N., S. Ghosh, D. L. Simmons, P. Tempst, H. C. Liou, D. Baltimore, and H. R. Bose, Jr.** 1991. Rel-associated pp40: an inhibitor of the rel family of transcription factors. Science **253**:1268–1271.
20. **Fan, C. M., and T. Maniatis.** 1991. Generation of p50 subunit of NF-κB by processing of p105 through an ATP-dependent pathway. Nature (London) **354**:395–398.
21. **Fischer, S. G.** 1983. Peptide mapping in gels. Methods Enzymol. **100**:424–430.
22. **Ghosh, S., and D. Baltimore.** 1990. Activation in vitro of NF-kappa B by phosphorylation of its inhibitor I kappa B. Nature (London) **344**:678–682.
23. **Ghosh, S., A. M. Gifford, L. R. Riviere, P. Tempst, G. P. Nolan, and D. Baltimore.** 1990. Cloning of the p50 DNA binding subunit of NF-κB: homology to rel and dorsal. Cell **62**:1019–1029.
24. **Grilli, M., J. J.-S. Chiu, and M. J. Lenardo.** 1993. NF-κB and Rel—participants in a multiform transcriptional regulatory system. Int. Rev. Cytol. **143**:1–62.
25. **Hansen, S. K., C. Nerlov, U. Zabel, P. Verde, M. Johnsen, P. A. Baeuerle, and F. Blasi.** 1992. A novel complex between the p65 subunit of NF-κB and c-Rel binds to a DNA element involved in the phorbol ester induction of the human urokinase gene. EMBO J. **11**:205–213.
26. **Haskill, S., A. A. Beg, S. M. Tompkins, J. S. Morris, A. D. Yurochko, A. Sampson Johannes, K. Mondal, P. Ralph, and A. S. Baldwin, Jr.** 1991. Characterization of an immediate-early gene induced in adherent monocytes that encodes I kappa B-like activity. Cell **65**:1281–1289.
27. **Hatada, E. N., A. Nieters, F. G. Wulczyn, M. Naumann, R. Meyer, G. Nucifora, T. W. McKeithan, and C. Scheidereit.** 1992. The ankyrin repeat domains of the NF-κB precursor p105 and the proto-oncogene bcl-3 act as specific inhibitors of NF-κB DNA binding. Proc. Natl. Acad. Sci. USA **89**:2489–2493.
28. **Henkel, T., U. Zabel, K. van Zee, J. M. Muller, E. Fanning, and P. A. Baeuerle.** 1992. Intramolecular masking of the nuclear location signal and dimerization domain in the precursor for the p50 NF-κB subunit. Cell **68**:1121–1133.
29. **Hohmann, H. P., R. Kolbeck, R. Remy, and A. P. van Loon.** 1991. Cyclic AMP-independent activation of transcription factor NF-κB in HL60 cells by tumor necrosis factors alpha and beta. Mol. Cell. Biol. **11**:2315–2318.
30. **Inoue, J., L. D. Kerr, A. Kakizuka, and I. M. Verma.** 1992. IκB gamma, a 70 kd protein identical to the C-terminal half of p110 NF-κB: a new member of the IκB family. Cell **68**:1109–1120.
31. **Inoue, J., L. D. Kerr, D. Rashid, N. Davis, H. R. Bose, Jr., and I. M. Verma.** 1992. Direct association of pp40/IκB beta with rel/NF-κB transcription factors: role of ankyrin repeats in the inhibition of DNA binding activity. Proc. Natl. Acad. Sci. USA **89**:4333–4337.
32. **Kawai, S., and M. Nishizawa.** 1984. New procedure for DNA transfection with polycation and dimethyl sulfoxide. Mol. Cell. Biol. **4**:1172–1174.
33. **Kawakami, K., C. Scheidereit, and R. G. Roeder.** 1988. Identification and purification of a human immunoglobulin-enhancer-binding protein (NF-κB) that activates transcription from a human immunodeficiency virus type 1 promoter in vitro. Proc. Natl. Acad. Sci. USA **85**:4700–4704.
34. **Kerr, L. D., J. Inoue, N. Davis, E. Link, P. A. Baeuerle, H. R. Bose, Jr., and I. M. Verma.** 1991. The rel-associated pp40 protein prevents DNA binding of Rel and NF-κB: relationship with IκB beta and regulation by phosphorylation. Genes Dev. **5**:1464–1476.
35. **Kieran, M., V. Blank, F. Logeat, J. Vandekerckhove, F. Lottspeich, O. Le Bail, M. B. Urban, P. Kourilsky, P. A. Baeuerle, and A. Israel.** 1990. The DNA binding subunit of NF-κB is identical to factor KBF1 and homologous to the rel oncogene product. Cell **62**:1007–1018.
36. **Kochel, T., J. F. Mushinski, and N. R. Rice.** 1991. The v-rel and c-rel proteins exist in high molecular weight complexes in avian and murine cells. Oncogene **6**:615–626.
37. **Kunsch, C., S. M. Ruben, and C. A. Rosen.** 1992. Selection of optimal κB/Rel DNA-binding motifs: interaction of both subunits of NF-κB with DNA is required for transcriptional activation. Mol. Cell. Biol. **12**:4412–4421.
38. **Lenardo, M. J., and D. Baltimore.** 1989. NF-κB: a pleiotropic mediator of inducible and tissue-specific gene control. Cell **58**:227–229.
39. **Lenardo, M. J., C. M. Fan, T. Maniatis, and D. Baltimore.** 1989. The involvement of NF-κB in beta-interferon gene regulation reveals its role as widely inducible mediator of signal transduction. Cell **57**:287–294.
40. **Liou, H. C., G. P. Nolan, S. Ghosh, T. Fujita, and D. Baltimore.** 1992. The NF-κB p50 precursor, p105, contains an internal IκB-like inhibitor that preferentially inhibits p50. EMBO J. **11**:3003–3009.
41. **Liptay, S., R. M. Schmid, N. D. Perkins, P. Meltzer, M. R. Altherr, J. D. McPherson, J. J. Wasmuth, and G. J. Nabel.** 1992. Related subunits of NF-κB map to two distinct loci associated with translocations in leukemia, NFKB1 and NFKB2. Genomics **13**:287–292.
42. **Meichle, A., S. Schutze, G. Hensel, D. Brunsing, and M. Kronke.** 1990. Protein kinase C-independent activation of NF-κB by tumor necrosis factor. J. Biol. Chem. **265**:8339–8343.
43. **Mercurio, F., J. DiDonato, C. Rosette, and M. Karin.** 1992. Molecular cloning and characterization of a novel Rel/NF-κB family member displaying structural and functional homology to NF-κB p50/p105. DNA Cell Biol. **11**:523–537.
44. **Mercurio, F., J. A. DiDonato, C. Rosette, and M. Karin.** 1993. p105 and p98 precursor proteins play an active role in NF-κB-mediated signal transduction. Genes Dev. **7**:705–718.
45. **Nabel, G., and D. Baltimore.** 1987. An inducible transcription factor activates expression of human immunodeficiency virus in T cells. Nature (London) **326**:711–713.
46. **Naumann, M., F. G. Wulczyn, and C. Scheidereit.** 1993. The NF-κB precursor p105 and the proto-oncogene product Bcl-3 are IκB molecules and control nuclear translocation of NF-κB. EMBO J. **12**:213–222.
47. **Neri, A., C. C. Chang, L. Lombardi, M. Salina, P. Corradini, A. T. Maiolo, R. S. Chaganti, and R. Dalla Favera.** 1991. B cell lymphoma-associated chromosomal translocation involves candidate oncogene lyt-10, homologous to NF-κB p50. Cell **67**:1075–1087.
48. **Neumann, J. R., C. A. Morency, and K. O. Russian.** 1992. A novel rapid assay for chloramphenicol acetyltransferase gene expression. Biotechniques **5**:444–448.
49. **Nolan, G. P., and D. Baltimore.** 1992. The inhibitory ankyrin and activator Rel proteins. Curr. Opin. Genet. Dev. **2**:211–220.
50. **Nolan, G. P., S. Ghosh, H. C. Liou, P. Tempst, and D. Baltimore.** 1991. DNA binding and IκB inhibition of the cloned p65 subunit of NF-κB, a rel-related polypeptide. Cell **64**:961–969.
51. **Ohno, H., G. Takimoto, and T. W. McKeithan.** 1990. The candidate proto-oncogene bcl-3 is related to genes implicated in cell lineage determination and cell cycle control. Cell **60**:991–997.
52. **Perkins, N. D., R. M. Schmid, C. S. Duckett, K. Leung, N. R. Rice, and G. J. Nabel.** 1992. Distinct combinations of NF-κB subunits determine the specificity of transcriptional activation. Proc. Natl. Acad. Sci. USA **89**:1529–1533.

53. **Rice, N. R., M. L. MacKichan, and A. Israel.** 1992. The precursor of NF-κB has IκB-like functions. Cell **71:**243–253.
54. **Ruben, S. M., P. J. Dillon, R. Schreck, T. Henkel, C. H. Chen, M. Maher, P. A. Baeuerle, and C. A. Rosen.** 1991. Isolation of a rel-related human cDNA that potentially encodes the 65-kD subunit of NF-κB. Science **251:**1490–1493.
55. **Ryseck, R. P., P. Bull, M. Takamiya, V. Bours, U. Siebenlist, P. Dobrzanski, and R. Bravo.** 1992. RelB, a new Rel family transcription activator that can interact with p50-NF-κB. Mol. Cell. Biol. **12:**674–684.
56. **Schmid, R. M., N. D. Perkins, C. S. Duckett, P. C. Andrews, and G. J. Nabel.** 1991. Cloning of an NF-κB subunit which stimulates HIV transcription in synergy with p65. Nature (London) **352:**733–736.
57. **Schreck, R., P. Rieber, and P. A. Baeuerle.** 1991. Reactive oxygen intermediates as apparently widely used messengers in the activation of the NF-κB transcription factor and HIV-1. EMBO J. **10:**2247–2258.
58. **Sen, R., and D. Baltimore.** 1986. Multiple nuclear factors interact with the immunoglobulin enhancer sequences. Cell **46:**705–716.
59. **Sen, R., and D. Baltimore.** 1986. Inducibility of kappa immunoglobulin enhancer-binding protein NF-κB by a posttranslational mechanism. Cell **47:**921–928.
60. **Shirakawa, F., and S. B. Mizel.** 1989. In vitro activation and nuclear translocation of NF-κB catalyzed by cyclic AMP-dependent protein kinase and protein kinase C. Mol. Cell. Biol. **9:**2424–2430.
61. **Staal, F. J., M. Roederer, and L. A. Herzenberg.** 1990. Intracellular thiols regulate activation of nuclear factor κB and transcription of human immunodeficiency virus. Proc. Natl. Acad. Sci. USA **87:**9943–9947.
62. **Storms, R. W., and H. R. Bose, Jr.** 1992. Alterations within pp59/v-rel-containing protein complexes following the stimulation of REV-T-transformed lymphoid cells with zinc. Virology **188:**765–777.
63. **Sun, S., P. A. Ganchi, D. W. Ballard, and W. C. Greene.** 1993. NF-κB controls expression of inhibitor IκBα: evidence for an inducible autoregulatory pathway. Science **259:**1912–1915.
64. **Urban, M. B., R. Schreck, and P. A. Baeuerle.** 1991. NF-κB contacts DNA by a heterodimer of the p50 and p65 subunit. EMBO J. **10:**1817–1825.
65. **Wulczyn, F. G., M. Naumann, and C. Scheidereit.** 1992. Candidate proto-oncogene bcl-3 encodes a subunit-specific inhibitor of transcription factor NF-κB. Nature (London) **358:**597–599.